# Relation Between Acid and Catalytic Properties of Chlorinated Gamma-Alumina. a 31p Mas Nmr and Ftir Investigation

D. Guillaume, S. Gautier, F. Alario, J. M. Deves



*Oil & Gas Science and Technology – Rev. IFP,* Vol. 54 (1999), No. 4, pp. 537-545


# Relation between Acid and Catalytic Properties of Chlorinated γ-Alumina

## A $^{31}$P MAS NMR and FTIR Investigation

D. Guillaume[1], S. Gautier[1], F. Alario[1] and J.-M. Devès[1]

*1 Institut français du pétrole, 1 et 4, avenue de Bois-Préau, 92852 Rueil-Malmaison Cedex - France*
*e-mail: serge.gautier@ifp.fr*

**Résumé — Relation entre les propriétés acides et catalytiques d'une alumine g chlorée. Étude par RMN RAM du $^{31}$P et par IRTF** — Cet article présente les effets de la chloration sur les propriétés acides de surface d'une alumine γ. L'utilisation combinée de l'infrarouge à transformée de Fourier (IRTF) et de la résonance magnétique nucléaire (RMN) du $^{31}$P en phase solide de la triméthylphosphine adsorbée permet de proposer un mécanisme de chloration. L'étude de la corrélation entre les propriétés acides de surface et les propriétés catalytiques d'alumines γ chlorées a été menée via la mise en œuvre d'une réaction catalytique test, le craquage du *n*-heptane dans les conditions du reformage catalytique. L'analyse des résultats obtenus a permis de relier les propriétés acides de surface, déterminées par RMN, au comportement catalytique (en termes d'activité et de sélectivité) des alumines γ chlorées. Cette corrélation a permis d'identifier quels sites sont responsables des réactions de craquage.

Mots-clés : RMN, infrarouge, TMP, thermodésorption, sites acides, distribution en force, alumine gamma, chloration, propriétés catalytiques, réactions de craquage.

**Abstract** — ***Relation between Acid and Catalytic Properties of Chlorinated γ-Alumina. A $^{31}$P MAS NMR and FTIR Investigation*** — *In this paper, we have studied the effect of chlorine on the surface properties of γ-alumina, especially on their acid properties. The use of FTIR spectroscopy and $^{31}$P MAS NMR of adsorbed trimethylphosphine allows to propose a chlorination mechanism. To correlate the surface properties of these chlorinated g-alumina with their catalytic properties, we have used a model reaction, the cracking of n-heptane under reforming conditions. The analysis of the correlation between acid properties determined by $^{31}$P MAS NMR and the catalytic results (in terms of activities and selectivities) allows to identify which sites are involved in the cracking reaction.*

*Keywords: NMR, infrared, TMP, thermodesorption, acid sites, stength distribution, gamma alumina, chlorine, catalytic properties, cracking reactions.*

## INTRODUCTION

The production of aromatic compounds in the refining and petrochemistry industry (products for the high octane gasolines and great intermediaries of synthesis) proceeds via catalytic reforming of paraffins. The most wanted reaction in reforming is the dehydrocyclization of *n*-paraffins in aromatics. This reaction proceeds mainly by metal-acid bifunctional mechanism [1, 2]. The catalysts, used actually in this aim, are constituted of well-dispersed metallic function (based on platinum) on a γ-alumina for which the acidity is promoted by around 1 wt% of chlorine [3]. Over such catalyst, it appears various cracking reactions, which make up the main parasitic reactions. These reactions must be limited because they lead to a loss of yield in reformat and decrease the production of hydrogen. The cracking reactions

have several possible origins : the metallic function (hydrogenolysis), the acidity of the support (acid cracking) and the temperature (thermal cracking).

The hydrogenolysis, which has been very studied over the past fifteen years, leads mainly to the formation of fuel gas ($C_1$, $C_2$). The activity of the metallic function in hydrogenolysis has been reduced by adding metal such as tin, indium or germanium [2].

The acid and thermal cracking reactions, as parasitic reactions, are less known. They distinguish themselves by the repartition of light hydrocarbons. Concerning the *n*-heptane cracking, the formation of products $C_3$-$C_4$ seems to result from acid cracking whereas the origin of products pairs $C_2$-$C_5$ and $C_1$-$C_6$ remains ill-definite. Indeed, the thermal cracking doesn't give many isomers with 5 and 6 carbon atoms. For the acid cracking of *n*-heptane in $C_1$-$C_6$ and $C_2$-$C_5$, the classic mechanisms imply reactional intermediaries (carbonium and primary carbenium ions) which existence is improbable over supports based on γ-alumina [4].

The lack of data in the literature on the formation of acid cracking products of naphtha over the support of reforming catalyst results mainly from the difficulty to characterize the surface acid properties of γ-alumina promoted by chlorine and to relate them to catalytic properties. In this paper, we clarify this situation by using different and complementary characterization techniques.

Aluminas promoted by chlorine at different contents have been prepared by chlorination of a γ-alumina with 1,2-dichloropropane at 500°C. The studied chlorine contents are close to these ones used industrially, between 0.8 wt% and 1.4 wt% of chlorine.

The effect of chlorine on the surface properties of γ-alumina, especially the nature, the amount and the strength of acid sites, has been measured by $^{31}P$ Magic Angle Spinning Nuclear Magnetic Resonance (MAS NMR) of adsorbed trimethylphosphine (TMP) and Fourier Transform InfraRed spectroscopy (FTIR) of surface hydroxyl groups. The cracking of *n*-heptane under reforming conditions has been used as a model reaction to correlate the surface properties of these chlorinated γ-alumina with their catalytic properties.

# 1 EXPERIMENTAL

## 1.1 Preparation of Chlorinated γ-Aluminas

A γ-$Al_2O_3$ sample (specific surface area of 193 $m^2g^{-1}$) was used. This alumina was first calcined at 530°C under flowing dry air for 2 h. The γ-$Al_2O_3$/Cl samples were obtained by oxychlorination with a $H_2O$-HCl-air stream. Gaseous HCl resulted of the decomposition in air of 1,2-dichloropropane at 500°C in $CO_2$, $H_2O$ and HCl. The samples were then calcined at 530°C under dry air for 2 h. At this step, chlorine content was about 1.4 wt%. Then chlorine content was lowered by calcining the sample at 530°C under air that contained about 20 000 wt ppm $H_2O$. Different chlorine contents were obtained by varying the time of calcination under wet air. This process of chlorination allowed the preparation of samples with a homogeneous repartition of chlorine at the surface of γ-alumina. The amount of chlorine was determined by X-ray fluorescence (XRF) and the specific surface areas of samples were measured by adsorption of nitrogen at –196°C. The specific surface areas of the chlorine modified aluminas are close to the specific area of the starting alumina material. According to the specific surface areas and chlorine loadings, the coverage in chlorine atoms was between 0.7 and 1.3 chlorine atom per $nm^2$ (Table 1).

TABLE 1

Samples characteristic

| Chlorine content (wt%) | Specific surface area ($m^2/g$) | Coverage in chlorine atom per $nm^2$ |
|---|---|---|
| 0 | 193 | 0 |
| 0.81 | 192 | 0.7 |
| 0.95 | 192 | 0.85 |
| 1.12 | 195 | 1.0 |
| 1.43 | 188 | 1.3 |

## 1.2 Characterization Techniques

### 1.2.1 Distribution of Hydroxyl Groups by FTIR Spectroscopy

Surface hydroxyl groups play an important role as surface functional groups in catalysis. OH groups represent diatomic surface oscillators, which give rise to typical infrared spectra. They can therefore be considered as intrinsic surface probes, the vibration frequencies contain informations on the coordination of the hydroxyl group hence on the local surface structure [5].

An infrared Fourier transform spectrometer (Digilab FTS80) was used for the analysis of the hydroxyl groups present at the surface of the solids. Samples were used as self-supporting wafers of 20 mg, activated *in situ* 2 h under vacuum of $10^{-6}$ mbar at 500°C. Spectra were recorded at room temperature with a resolution of 4 $cm^{-1}$ and the number of scans was fixed to 300.

### 1.2.2 Strength Distribution of Acid sites by Thermodesorption of Trimethylphosphine (TMP) Followed by $^{31}P$ MAS NMR

*Principle*

Among the surface acidity characterization methods of solid state materials, solid state NMR spectroscopy of basic probe molecules has emerged as a promising approach to evaluate the type and the number of acid sites on zeolites and other

aluminosilicates. Nitrogen-15 bases, including ammonia, pyridine, trimethylamine and *n*-butylamine have been effectively used [6-9]. However, the small magnetogyric ratio of $^{15}N$ results in sensitivity problems. These difficulties have been overcome by adopting $^{31}P$-containing probe molecules. The $^{31}P$ nucleus is an attractive candidate for surface acidity characterization studies as it possesses a large chemical shift range and it is, from an NMR point of view, a sensitive nucleus (100% natural abundance). Among the possible phosphored bases, TMP has been employed to probe Brönsted and Lewis acidity in zeolites [10-13] and other materials [14-18]. Because of its high basic strength (TMP basicity is about 1000 times greater than that of pyridine) and its rather small size, this probe is able to be adsorbed on a large amount of the solid acid sites. On the other hand, because of its air sensitivity, all experiments must then be done under controlled atmosphere. In a previous paper [19], we have demonstrated that $^{31}P$ MAS NMR, combined with thermodesorption, is a powerful method to determine the strength distribution of Brönsted and Lewis sites on this type of samples.

The $^{31}P$ NMR spectra of TMP adsorbed on γ-alumina supports contain two main peaks. A large one with a maximum close to –50 ppm attributable to Lewis acid sites, and a smaller one located at about –5 ppm due to Brönsted acid sites [18]. Weak resonances between 20-30 ppm and 50-70 ppm can be detected. They have been attributed to oxidised TMP adsorbed on Lewis acid sites [19].

The thermodesorption under vacuum of the TMP adsorbed at the catalyst surface enables to evaluate the strength of acid sites. TMP adsorbed on a strong acid site is more stable than one adsorbed on a weak acid site, and is more difficult to desorb. As high temperatures stimulate evacuation of the adsorbed molecules from acid sites, those at weaker sites will be evacuated preferentially. Thus, the proportion of adsorbed base evacuated at various temperatures can give a measure of acid strength distribution. Figure 1 shows, for example the $^{31}P$ NMR spectra of TMP species adsorbed on γ-alumina pretreated at 530°C. TMP was adsorbed at room temperature and then evacuated at 100, 200 and 350°C. A narrow structure appears for samples degassed at high temperature. This behaviour has been demonstrated to be characteristic of a J-coupling between aluminium and phosphorus [20, 21].

The amount of phosphorus on each samples can be determined by XRF. During XRF analysis, samples have been put under air, leading to an oxidation of the adsorbed TMP. Previous experiments have shown that TMP initially adsorbed on Brönsted acid sites is desorbed when oxidised. This is not the case for TMP initially adsorbed on Lewis acid sites [19]. Consequently, the only measured phosphorus by XRF correspond to oxidised trimethylphosphine species adsorbed on Lewis acid sites. A good linear correlation is effectively obtained between the phosphorus content, determined by XRF, and the NMR signal, which are assigned to oxidised and non-oxidised TMP species adsorbed on Lewis acid sites (Fig. 2). Then XRF measurements allow to calculate the total number of Lewis acid sites per area unit. As NMR spectra have been recorded under quantitative conditions, it is possible to evaluate Lewis and Brönsted sites distribution owing to their acid strength.

*Sample Preparation*

Samples were pretreated for 2 h under flowing helium at 530°C and transferred into an adsorption cell in an air free glove box. Vacuum was maintained in the cell at 7.5 $10^{-5}$ torr

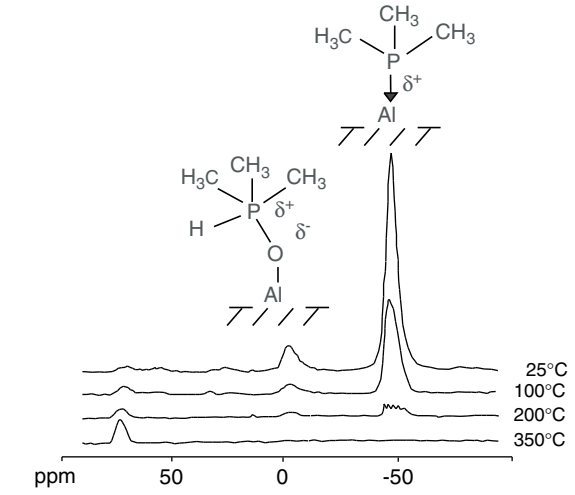


Figure 1

Effect of the desorption temperature on the $^{31}P$ MAS NMR spectra of $(CH_3)_3P$ in γ-alumina pretreated at 530°C [19].

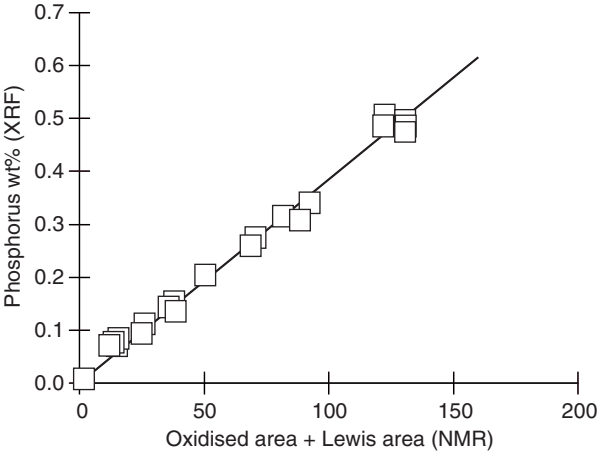


Figure 2

Correlation betwen the phosphorus content and the resonance area sum assigned to oxidised and non-oxidised TMP species adsorbed on Lewis acid sites [19].

overnight. Trimethylphosphine (Aldrich) was introduced from vapor phase at room temperature up to saturation and allowed to equilibrate for 0.5 h. Samples were degassed under vacuum at 25, 100, 200 and 350°C. Samples were then transferred into a 4 mm ceramic zirconia NMR rotor in an air free glove box. To minimize oxidation, NMR spectra were recorded immediately after.

*NMR Measurements*

$^{31}P$ MAS NMR spectra were recorded using a Brüker MSL 400 spectrometer, the $^{31}P$ resonance frequency was 162 MHz. $^{31}P$ chemical shifts were reported relative to 85% $H_3PO_4$. Direct 90° pulses were used with a pulse width of 4 µs. $^{31}P$ MAS NMR spectra were recorded with proton inverse gated decoupling [22]. Typical spinning rate was 12 kHz. The phosphorus $T_1$ (longitudinal relaxation time) for adsorbed species is relatively short, less than 1 s, and the repetition rate was 5 s, thus spectra were recorded under appropriate conditions for direct quantification. The number of scans per acquisition was 1000.

### 1.2.3 n-heptane Cracking

Heptane cracking tests have been performed in a fixed bed continuous flow "Catatest" unit under hydrogen pressure. Experimental conditions were total pressure of 3 bar, reaction temperature of 510°C, hourly space velocity (HSV) between 0.2 and 5 $h^{-1}$, hydrogen/heptane molar ratio of 4. The amount of catalyst used was 20 g. Prior to catalytic tests, the samples were activated *in situ* for 2 h under flowing helium at 530°C.

The reaction products were analysed by a gas chromatograph equipped with a flame ionization detector. Separation of products was carried out using a plot alumina capillary column with a KCl phase (50 m length).

From the chromatographic data, the total activity, the activities and the selectivities towards the different reaction products were calculated. As the selectivity is a function of the conversion level, a meaningful comparison of selectivities can only be made at similar conversion levels. Such conditions were achieved by carefully adjusting the hourly space velocity to compare the selectivities at 20% $nC_7$ conversion. For the comparison of activities, $nC_7$ cracking tests were performed in the same experimental conditions for the different samples.

## 2 RESULTS

### 2.1 Strength Distribution of Acid Sites by $^{31}P$ MAS NMR of Adsorbed TMP

The strength distributions of acid sites on γ-alumina and chlorinated γ-alumina are presented in Figure 3. For each acidity type (Lewis or Brönsted), four categories of sites are proposed. Each of them corresponds to a desorption temperature interval of TMP.

For Lewis acid sites, the chlorination increases the number of sites adsorbing TMP beyond 200°C and decreases the number of sites desorbing the TMP up to 200°C. We will call "strong sites" the ones TMP is desorbed from above 200°C and "weak sites" up to 200°C (Fig. 4). As the increase of the number of strong Lewis acid sites is in the same order of magnitude as the decrease of the number of weak Lewis acid

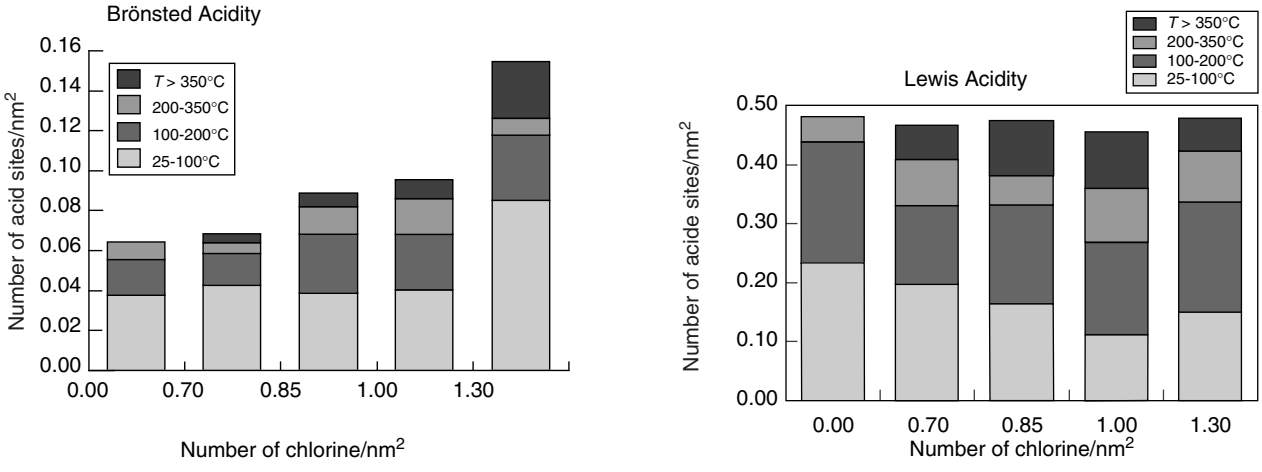


Figure 3

Strength distributions of Brönsted and Lewis acid sites as a function of γ-alumina chlorine content (acid strength is determined from TMP desorption temperature levels).

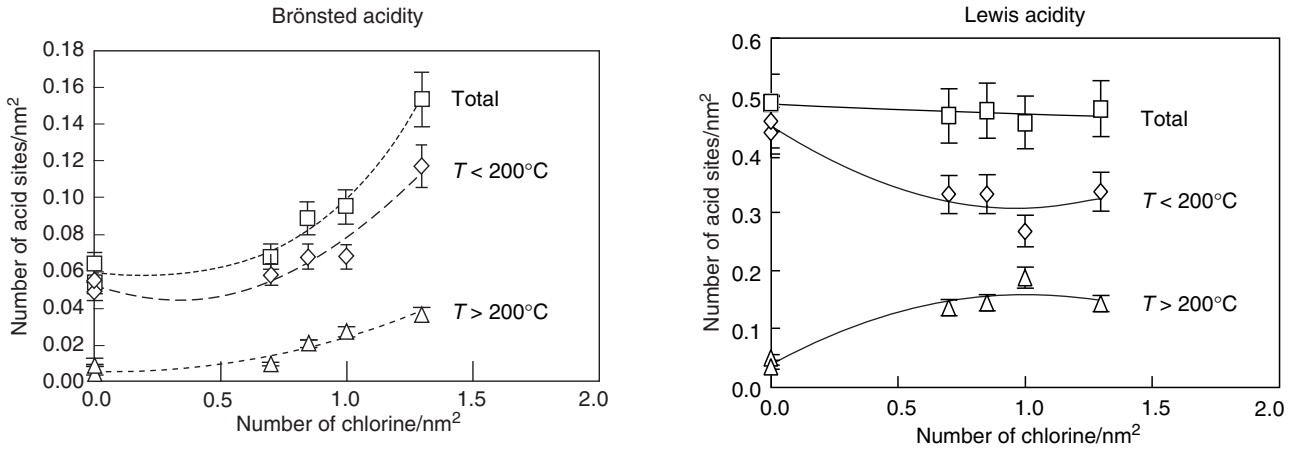


Figure 4

Chlorine effect on the Brönsted and Lewis acidity levels of γ-alumina (weak and strong acid strength sites are determined from desorption temperature of TMP inferior to 200°C and superior to 200°C respectively).

sites, the total amount of Lewis acid sites remains stable. A similar evolution has been already observed by FTIR spectroscopy of adsorbed pyridine on a γ-alumina chlorinated with HCl at 200°C. Melchor [23] has shown that the number of Lewis acid sites desorbing pyridine at temperature higher than 250°C increases with chlorine addition to the detriment of Lewis acid sites desorbing pyridine at an inferior temperature.

The modification of the strength distribution of Brönsted acid sites on γ-alumina with the chlorine addition is due to the creation of sites of both type of acidity (weak and strong). Consequently, the total amount of Brönsted acid sites increases with the addition of chlorine.

In summary, the alumina chlorination increases the number of Brönsted acid sites and the number of strong Lewis acid sites to the detriment of the number of weak Lewis acid sites.

## 2.2 Surface Hydroxyl Groups by FTIR Spectroscopy

The influence of chlorine level on the surface hydroxyl groups of the starting γ-alumina has been followed by IR spectroscopy in the region of O-H stretching fundamental vibrations (Fig. 5). The differential IR spectra, presented also in figure 5, describe the evolution of surface hydroxyl groups with the chlorine level.

The infrared spectrum of the starting γ-alumina exhibits four bands located at 3794, 3775, 3730 and 3686 $cm^{-1}$. The addition of 0.7 atom of chlorine per $nm^2$ leads to the total disappearance of bands of highest wave number (3794 and 3775 $cm^{-1}$). Above 0.7 atom of chlorine, the intensity of the band at 3730 $cm^{-1}$ decreases. The band at 3686 $cm^{-1}$ shows an increase of its width for the highest chlorine level (1.3 atom per $nm^2$). This is due to a new band at 3661 $cm^{-1}$.

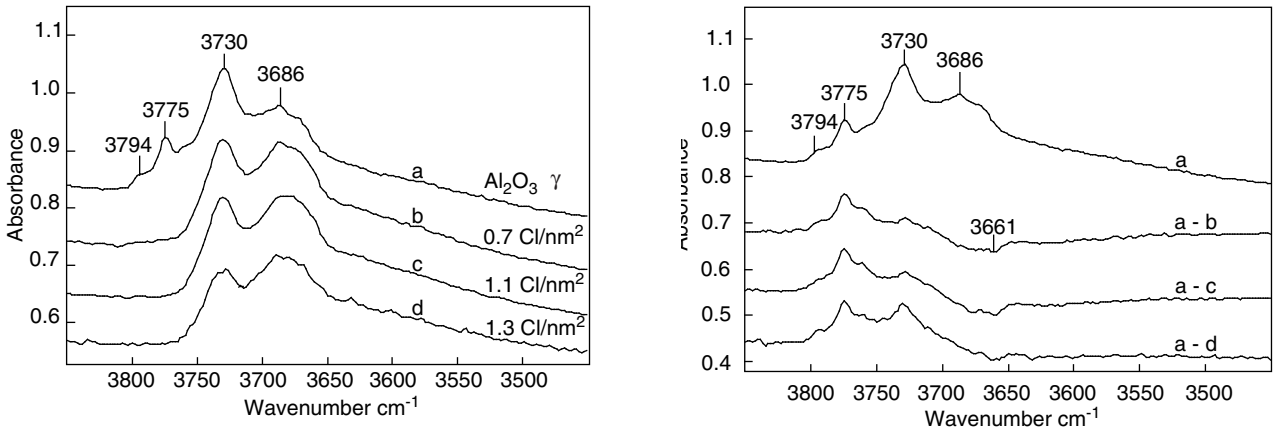


Figure 5

IR spectra in the OH absorption range of chlorinated alumina samples.

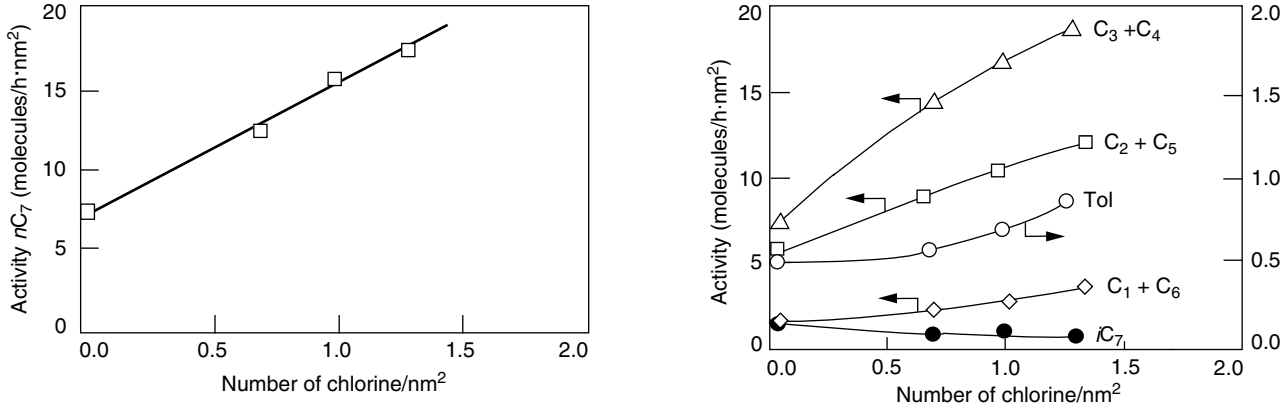


Figure 6

Activities of chlorinated γ-alumina in $nC_7$ cracking (same experimental conditions, HSV = 1 h–1).

## 2.3 *n*-heptane Cracking

The addition of chlorine increases the global activity of the catalysts. This increase is mainly due to an higher production of cracking products (Fig. 6). The comparison of catalytic and acid properties of chlorinated γ-aluminas suggests that the cracking reactions of $nC_7$ have for origin the acidity of support. The assumption of a thermal cracking in the formation of $C_1$-$C_6$ and $C_2$-$C_5$ product couple can be discarted.

Morever, at a same $nC_7$ conversion level, the chlorination of γ-alumina leads to an increase of the selectivity of $C_3$-$C_4$ products couple and a decrease of selectivities in isomerization and cyclization products. We can notice that the products distribution remains stable as soon as 0.7 atom of chlorine per nm$^2$ is added (Fig. 7).

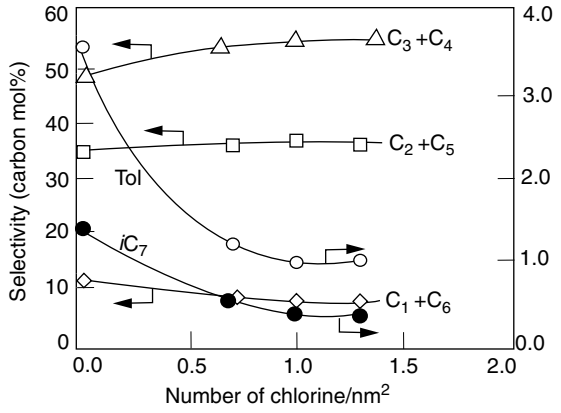


Figure 7

Selectivities of chlorinated γ-alumina at 20% conversion level in $nC_7$ cracking.

# 3 DISCUSSION

## 3.1 Model of Chlorination

The effect of chlorine on the nature and the environment of acid sites has been examinated by taking into account the configuration of adsorption sites which come from the regular dehydroxylation of the preferentially exposed crystallographic planes at the surface of cristallites of γ-alumina. According to Nortier [24], the (110) faces are the most abundant on the γ-alumina. There are two types of layers containing two different cation distributions present in the spinel lattice parallel to the (110) plane, the C and D layers. In Figure 8 are represented the different hydroxyl types, proposed by Lavalley [25], present on the completely rehydroxylated C and D-layers. Complete rehydroxylation of the C-layer leads to type Ia [OH-$Al_{IV}$], type IIb [$Al_{VI}$-OH-$Al_{VI}$] and type III' [$Al_{IV}$-OH-$(Al_{VI})_2$]. On the D layer, three types of OH groups are expected: type geminal [$(OH)_2$-$Al_{VI}$], type IIa [$Al_{IV}$-OH-$Al_{VI}$], type III [OH-$(Al_{VI})_3$].

Taking into consideration that the regular dehydroxylation process is governed by the relative basicity and protonic acidity of neighboring OH [26], Lavalley [25] describe four adsorption sites, two on C-layer (1c and 2c sites) and two on D-layer (1d and 2d sites) (fig. 8).

### 3.1.1 On C-Layer of (110) Plane of Alumina Spinel Structure

From experiments of $^{27}$Al MAS RMN by cross-polarization of adsorbed $NH_3$, Coster [27] has determined the coordination of aluminium cations responsible for the Lewis acidity at the surface of a γ-alumina pretreated at high temperature. No tricoordinated aluminium cation in tetraedral position (anionic vacancy which exposes an aluminium cation in a tetraedral position) is observed. Only tetracoordinated or pentacoordinated aluminium cations in octaedral position

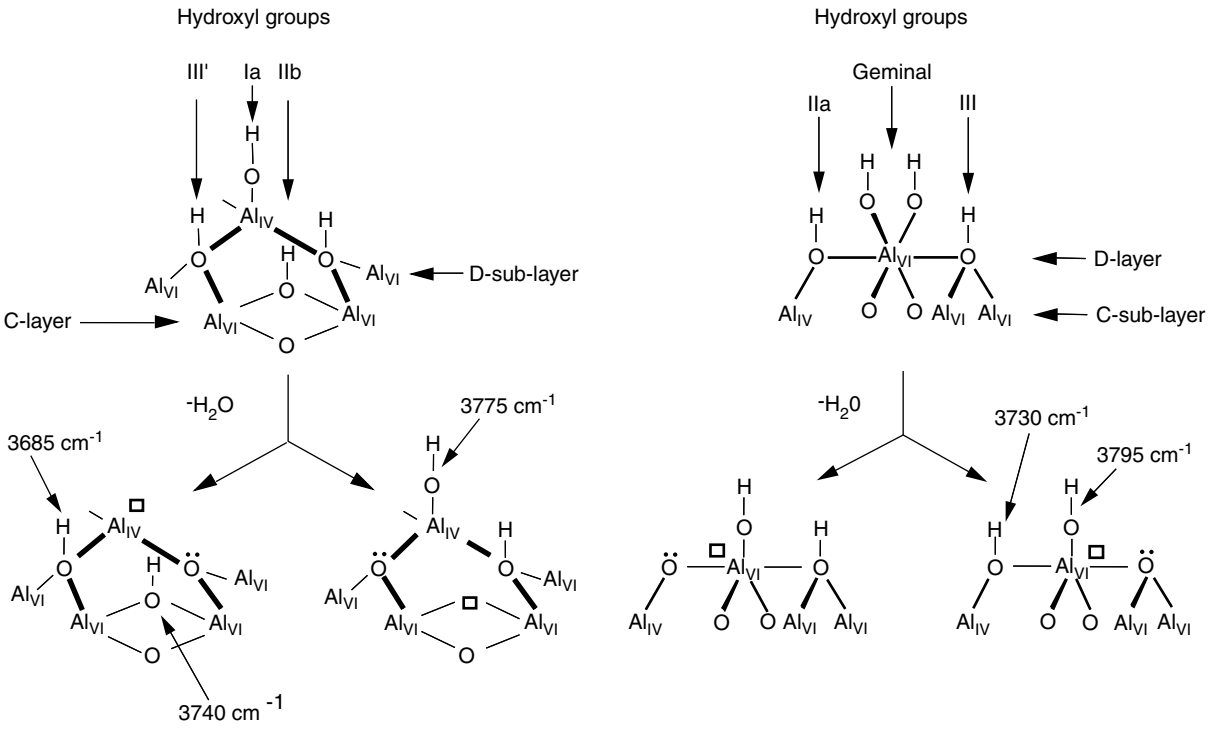


Figure 8

OH vibration frequencies for different adsorption sites issued from the regular dehydroxylation of (110) plane of alumina spinel structure [25] ($Al_{VI}$ and $Al_{IV}$: aluminium cation in octahedral and tetrahedral position respectively; ❒: anionic vacancy, Ö: coordinatively unsaturated oxygen anion).

would be responsible for the Lewis acidity. According to these results, the 1c adsorption site doesn't exist. Consequently, only the 2c adsorption site has been considered in the chlorination process of the C-layer. A substitution of basic OH group by HCl gaz is proposed to account for the disappearance of the high-frequency band at 3775 $cm^{-1}$ (Fig. 9). Because of its electronegatif character, chlorine increases the strength of adjacent acid sites by inductive effect. So, the increase of the width of the band at 3685 $cm^{-1}$ would result from the strengthening of the acid character of type III' hydroxyl group.

In accordance with the IR studies, NMR results point out an increase of the amount of strong Brönsted sites. In addition, NMR shows also that some of weak Lewis sites became strong Lewis sites (Fig. 9).

#### 3.1.2 On D-Layer of (110) Plane of Alumina Spinel Structure

IR and NMR results suggest a chlorination process with gaseous HCl by heterolytic dissociative adsorption of HCl with concerted desorption of water on the 2d adsorption site. Indeed, an adsorption mechanism on 1d site will lead to a creation of an neutral hydroxyl group (band at 3730 $cm^{-1}$) and a decrease of the number of hydroxyl groups bridged to three alumina (band at 3685 $cm^{-1}$, whatever could be the type of alumina [25]). IR spectra doesn't show such evolution. On 2d adsorption site, this process leads to a diminution of the number of basic (3795 $cm^{-1}$) and neutral (3730 $cm^{-1}$) hydroxyl groups. IR spectra confirm this evolution. In agreement with NMR results, this mechanism leads to a creation of strong Brönsted and Lewis sites (Fig. 9).

In summary, IR and NMR results allowed to assume that chlorination process occurs only on two of the four possible adsorption sites of (110) plane. On C-layer, it proceeds via a substitution of basic hydroxyl groups on 2c adsorption sites. On D-layer, it proceeds via a heterolytic dissociative adsorption of HCl with concerted desorption of water on 2d adsorption sites.

### 3.2 Relationship between the Acid and Catalytic Properties

The analysis of the evolution of acidic properties of chlorinated γ-alumina, determined by NMR, allows to explain the origin of cracking products of n-heptane.

Figure 10 shows that there is no correlation between the global activity and the total number of acid sites (Brönsted and Lewis). In opposition, a good relationship has been found by taking into account only the strong Lewis sites plus the total number of Brönsted sites. This suggests that the

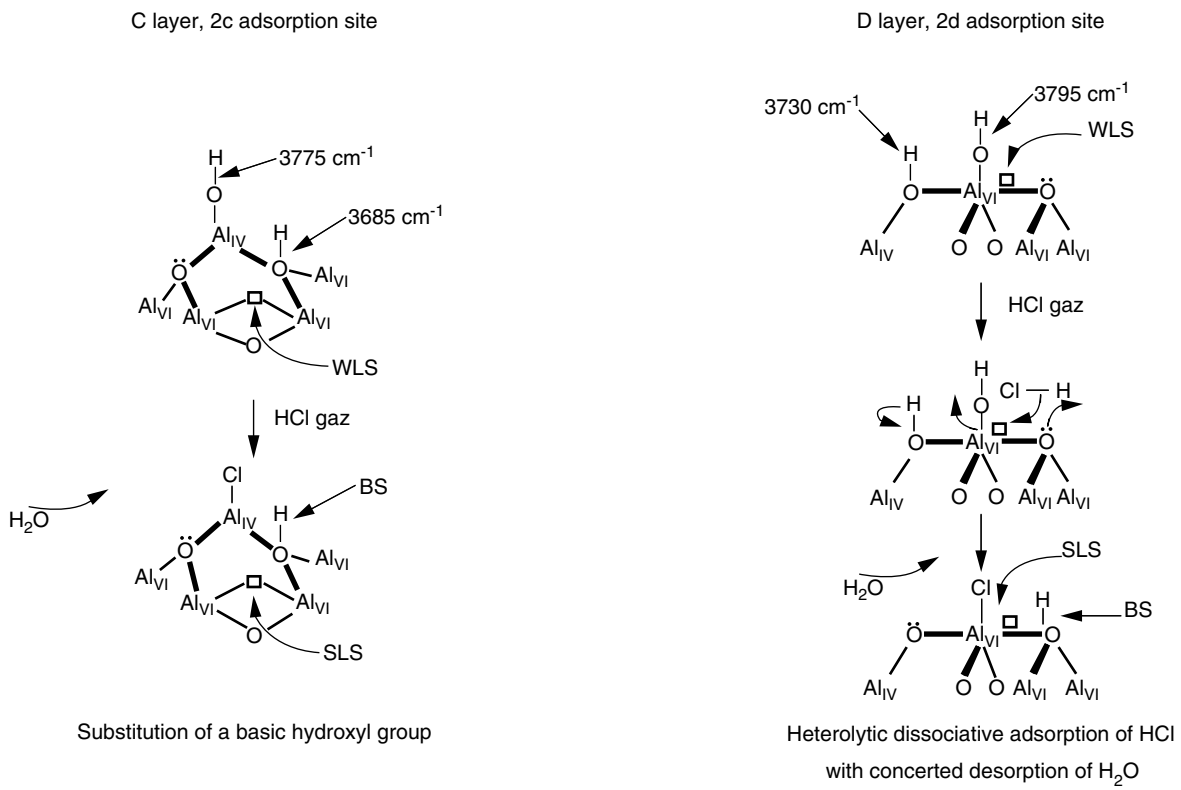


Figure 9

Chlorination process by gaseous HCl on γ-alumina. WLS: weak Lewis sites, SLS: strong Lewis sites, BS: Brönsted sites.

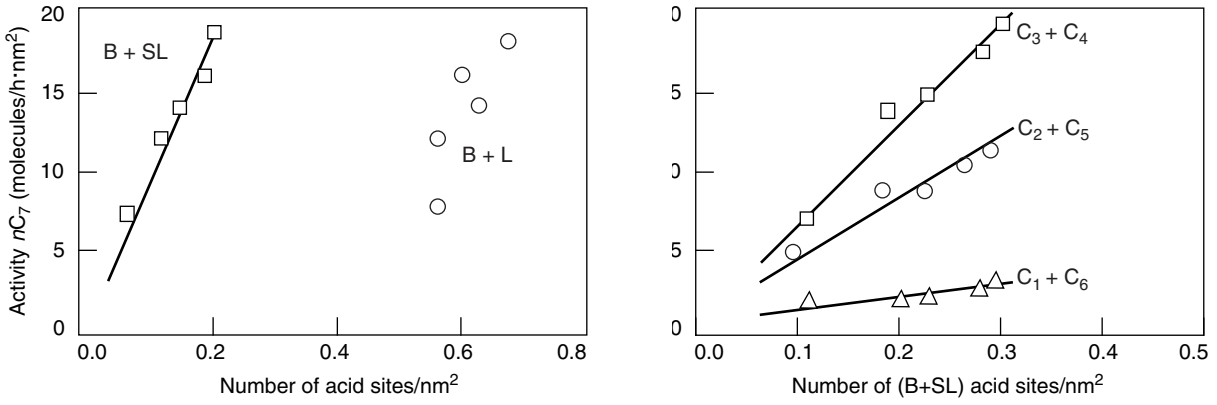


Figure 10

Relationship between activity and number of acid sites.

weak Lewis acid sites don't participate to the conversion of *n*-heptane. In the same manner, the best correlations have been observed between the cracking activities of each product couple and the sum of the total number of Brönsted and strong Lewis sites (Fig. 10). These results seems to show that the formation of $C_1$-$C_6$, $C_2$-$C_5$ and $C_3$-$C_4$ product couples are due to the same acid sites. If, in literature, the participation of Brönsted and/or Lewis acid sites in the formation of $C_3$-$C_4$ couple by β-scission of heptylcarbenium ions can be considered, the situation is not so clear for the two others product couples. Indeed, considerations on the stability of reactional intermediaries suggest a cracking by radicalar β-scission mechanism [4]. This mechanism concerns only Lewis acid sites and not the Brönsted acid sites.

In fact, the good correlation obtained when including the Brönsted sites for the $C_1$-$C_6$ and $C_2$-$C_5$ formation doesn't

imply necessarely a straightforward participation of Brönsted acid sites in this type of cracking. It is wellknown that more the cracked and crackable species are stable more the *n*-heptane cracking is high. Such species are obtained by a previous isomerization step on Brönsted acid sites. This justifies that in order to correctly explain the amount of cracking products the amount Brönsted sites has to be taken into account even if they don't directly participate to the cracking step.

According to Figure 7, the increase of the selectivity in $C_3$-$C_4$ is in the same order of magnitude as the decrease of selectivities in toluene and $iC_7$, as soon as chlorine is added on γ-alumina. A similar evolution has been observed when γ-alumina is modified by addition of silicon [4]. This has been explained by a different strength of acid sites of the same nature (Brönsted acid sites) required for the formation of cyclization, isomerization and $C_3$-$C_4$ cracking products. As for silicon modified γ-aluminas, the proportion of cracking Brönsted acid sites (the strongest acid sites), on chlorinated γ-aluminas, would be higher than the ones of Brönsted acid sites leading to the formation of isomerization and cyclisation products (weaker acid sites).

## CONCLUSION

The thermodesorption of TMP followed by $^{31}$P MAS NMR is a powerful method for the study of acid properties of materials such as chlorinated γ-alumina. This method is able to determine the strength distribution of acid sites, either Brönsted or Lewis sites. The number of acid sites revealed by TMP is given by the phosphorous content measured on samples by X-ray fluorescence.

The characterization of acid sites by $^{31}$P NMR combined with FTIR spectroscopy of hydroxyl groups has allowed us to propose chlorination mechanisms of γ-alumina with gaseous HCl. Chlorination process occurs only on two of the four possible adsorption sites of (110) plane. On C-layer, a mechanism by substitution of basic hydroxyl groups is proposed on a 2c adsorption site. On D-layer, a heterolytic dissociative adorption of HCl with concerted desorption of water occurs on a 2d adsorption site.

The relationship between the acid caracteristics of chlorinated γ-alumina and their catalytic behavior in the *n*-heptane conversion has been studied. We have identified which acid sites are involved in the cracking process. To correctly predict the activity of a catalyst one should not take into account just the strong Lewis acid sites but also the Brönsted acid sites. We suggest that this sites are involved in a previous isomerization step leading to more crackable species. It implies that the catalytic process is composed by two steps, an isomerisation of *n*-heptane on the Brönsted acid sites followed by the cracking step on the strong Lewis acid sites.

## REFERENCES


1 Gates, B.C., Katzer, J.R. and Schuit, G.C.A. (1979) Chemistry of Catalytic Processes. *Chem. Eng. Series*, Mc Graw Hill, New York.

2 Parera, J.M. and Figoli, N.S. (1995) in: *Catalytic Naphtha Reforming, Science and Technology*, Part II, Eds. G.J. Antos, A.M. Aitani and J.M. Parera, Ch. 3, p. 4, Marcel Dekker, New York.

3 Boitiaux, J.P., Devès, J.M., Didillon, B. and Marcilly, Ch. (1995) in: *Catalytic Naphtha Reforming, Science and Technology*, Part II, Eds. G.J. Antos, A.M. Aitani and J.M. Parera, Ch. 4, p. 79, Marcel Dekker, New York.

4 Guillaume, D. (1997) *Thesis* No. 44186, Institut français du pétrole, France.

5 Boehm, H.P. and Knözinger, H. (1983) in: *Catalysis, Science and Technology*, **4**, Eds. J.R. Anderson and M. Boudart, Ch. 2, p. 39, Springer-Verlag, New York.

6 Earl, W.L., Fritz, P.O., Gibson, A.A.V. and Lunsford, J.H. (1987) *J. Phys. Chem.,* 91, 2091.

7 Ripmeester, J.A. (1983) *J. Am. Chem. Soc*., 105, 2925.

8 Maciel, G.E., Haw, J.F., Chuang, I.S., Hawkins, B.L., Early, T.E., McKay, D.R. and Petrakis, L. (1983) *J. Am. Chem. Soc.,* 105, 5529.

9 Haw, J.F., Chuang, I.S., Hawkins, B.L. and Maciel, G.E. (1983) *J. Am. Chem. Soc.,* 105, 7206.

10 Lunsford, J.H., Rothwell, W.P. and Shen, W.X. (1985) *J. Am. Chem. Soc,.* 107, 1540.

11 Lunsford, J.H., Tutunjian, P.N., Chu, P.J., Yeh, E.B. and Zalewski, D.J. (1989) *J. Phys. Chem.,* 93, 2590.

12 Bendada, A., De Rose, E.F. and Fripiat, J.J. (1994) *J. Phys. Chem.,* 98, 3838.

13 Yong, H., Coster, D., Chen, F.R., Davis, J.G. and Fripiat, J.J. (1993) in: *New Frontiers in Catalysis, Studies in Surface Science and Catalysis*, **75 B**, Eds. L. Guczi, F. Solymosi and P. Tétényi, p. 1159, Elsevier, Amsterdam.

14 Baltusis, L., Frye, J.S. and Maciel, G.E. (1987) *J. Am. Chem. Soc.,* 109, 40.

15 Coster, D., Bendada, A., Chen, F.R. and Fripiat, J.J. (1993) *J. Catal.,* 140, 497.

16 Sheng, T.C., Kirszensztejn, P., Bell, T.N. and Gay, I.D. (1994) *Catal. Lett.,* 23, 119.

17 Sheng, T.C. and Gay, I.D. (1994) *J. Catal.,* 145, 10.

18 Sang, H., Chu, H.Y. and Lunsford, J.H. (1994) *Catal. Lett*., 26, 235.

19 Guillaume, D., Gautier, S., Despujol, I., Alario, F. and Beccat, P. (1997) *Catalysis Letters,* 43, 213.

20 Chu, P.J., Lunsford, J.H. and Zalewski, D.J. (1990) *J. Magn. Reson.,* 87, 68.

21 Chu, P.J., De Mallman, A. and Lunsford, J.H. (1991) *J. Phys. Chem.,* 95, 7362.

22 Brau, S., Kalinowski, H.O. and Berger, S. (1996) *100 and More Basic NMR Experiments*, *A Practical Course*. VCH Publishers, New York, 1996) Ch. 4.

23 Melchor, A.E. (1983) *Thesis* No. 83-60, Université Lyon I, France.

24 Nortier, P., Fourre, P., Mohammed Saad, A.B., Saur, O. and Lavalley, J.C. (1990), *Appl. Catal.,* 61, 141.

25 Mohammed Saad, A.B., Ivanov, V.A., Lavalley, J.C., Nortier, P. and Luck, F. (1993), *Appl. Catal*., 94, 71.

26 Knözinger, H. and Ratnasamy, P. (1978) *Catal. Rev. Sci. Eng*., 17, 31.

27 Coster, D., Blumenfeld, A.L. and Fripiat, J.J. (1994) *J. Phys. Chem.,* 98, 6201.

28 Tiong Sie, S. (1992) Ind. Eng. Chem. Res., 31,1881.


*Final manuscript received in May 1999*